GROWTH KINETICS FOR THE PRECIPITATION OF ZIRCONIUM HYDROXIDE FROM AQUEOUS ZIRCONIUM AND TIN BEARING SOLUTIONS BY THE ADDITION OF AMMONIUM HYDROXIDE[a]

WINCO--11562

DE92 017480

by

Thomas E. Carleson
Department of Chemical Engineering
University of Idaho
Moscow, Idaho

Nathan A. Chipman
Westinghouse Idaho Nuclear Company
Idaho National Engineering Laboratory
Idaho Falls, Idaho

ABSTRACT

The precipitation of zirconium hydroxide from an aqueous solution of ammonium hexafluorozirconate occurs rapidly upon addition of ammonium hydroxide. Experimental data indicate growth and nucleation rates between 0.06 and 0.28 microns/minute and around 10×10^7 number/L-min, respectively. Experiments with a mixed suspension mixed product removal crystallizer for concentrations of reactants of about 0.05 M ammonium hexafluorozirconate precipitating with 0.002 M ammonium hydroxide showed apparent nonlinear growth rates in some cases but not others. Batch studies indicated that growth rate dispersion is probably not present. When the ASL nonlinear model was used to fit the data, the power coefficient obtained was greater than 1, in disagreement with theory. In addition, for some of the data "S" shaped curves of the logarithm of the cumulative number greater than versus size were obtained. These curves can not be fit by the ASL model. A program developed at the University of Arizona was used to simulate the crystallization runs. The program results indicated that some of the nonlinear behavior may be attributed to ---- >

[a] Work supported by the U.S. Department of Energy Assistant Secretary for Defense Programs, under DOE Contract No. DE-AC07-ID12435.

DISCLAIMER

transient conditions. Experimental data also illustrated this behavior. The effect of trace amounts of tin fluoride (0.008 M) on the nucleation and growth kinetics was also evaluated. For some residence times, the presence of tin resulted in reduced median particle diameters, higher growth rates, and lower number counts.

INTRODUCTION AND BACKGROUND

In its effort to reduce the amount of high-level radioactive waste produced from reprocessing defense nuclear fuels, Westinghouse Idaho Nuclear Company, Inc., operating contractor of the Department of Energy's Idaho Chemical Processing Plant, has evaluated several processes to remove zirconium and/or other fuel components such as tin, a major alloying component, from liquid waste streams. In some of these processes, zirconium and other metals are precipitated by the addition of ammonia gas or ammonium hydroxide. These precipitation methods have the potential to reduce the high-level radioactive waste volumes by about 30% compared to the present process.[1]

The evaluation of these processes required the study of the nucleation and growth kinetics of zirconium hydroxide.[2] Zirconium fluoride was dissolved in an ammonium fluoride solution to form hexafluorozirconate anions. The addition of hydroxide either as ammonia gas or ammonium hydroxide resulted in the formation of a dense, white precipitate of zirconium hydroxide. The present report summarizes particle size measurements for the precipitation process and presents nucleation and growth rates based upon crystallization theory.

The unsteady-state crystal number balance for a mixed suspension mixed product removal (MSMPR) crystallizer is:

$$(1) \qquad \frac{\partial n}{\partial t} + G\left(\frac{\partial n}{\partial L}\right) + n\left(\frac{\partial G}{\partial L}\right) + \frac{n}{t^*} = 0$$

where n is the population or number density of the particle of size L, G is the growth rate, and t* is the residence time. If the McCabe linear growth law, i.e., growth rate is independent of size, is assumed, the steady-state solution to this equation for the nuclei concentration, is:

$$(2) \qquad n = n_0 \exp(-L/Gt^*)$$

where n_0 is the nuclei (L = 0) population density. A plot of ln(n) versus L will then yield a slope and intercept from which n_0 and G may

be found. Similarly, the number distribution can be integrated over L between a given size and infinity to result in:

$$N_L = (n_o Gt^*)\exp(-L/Gt^*) \quad (3)$$

where N_L is the cumulative number of particles greater than size L. A semi-logarithmic plot can be made to evaluate G and n_o.

Unsteady-state solutions to the same equation (assuming linear growth) have also been found.[3,4,5,6] The unsteady-state solutions exhibit a modified second order response of number density to changes in flow rate. Population of the smallest sizes changes almost immediately to reflect changes in residence time in accordance with the above equations. For example, for an increase in flow rate, the resulting initial higher solution concentration in the MSMPR vessel results in a higher supersaturation and consequently a rise in nucleation and growth rates. This results in a high concentration of small particles. However, due to this sudden increase in nuclei concentration, the supersaturation ratio decreases. Consequently a portion of the large number of small particles are washed out and not replenished by nucleation. The rest grow and this number of growing particles proceeds up the size range with time. Meanwhile the population of smaller sizes decreases toward its steady-state value. The peak in population density is dampened as it travels up the particle size distribution to larger sizes.[4] The largest sizes may see a washout effect for an increase in flow rate initially and then an almost first order response to result in lower number densities.[3] Approximately 10 residence times are required for steady-state for the larger (greater than 500 micron) particle sizes.

The linear growth model, however, may not be applicable to all crystal size distributions. The microscopic processes occurring at the crystal surfaces due to variations in number, size, and location of the screw dislocation at different crystal faces may result in growth rate dispersion.[7] These may be caused by contact of the growing crystals with the vessel walls or other crystals. This results in a constant time averaged growth rate but one which varies with each individual crystal.[8] Alternatively, in another proposed mechanism the crystals are born with a characteristic distribution of growth rates, but individual crystals retain a constant growth rate throughout their residence time in the crystallizer.[9]

There are many semi-empirical models for non-linear growth kinetics. One of these, the ASL equation[10] is:

$$G = G_o(1 + aL)^b \quad (4)$$

This model allows for a power law dependence of G upon L. According to the theory b must be less than one to allow this distribution to fit the population balance equation. The model, however, is semi-empirical and the coefficients often do not have any fundamental meaning. The ASL model is used to correlate data where the logarithm of the cumulative number of particles greater than a given size appears to decrease with particle size in a non-linear fashion. This form of the equation is:

$$N_L = N_T \exp\left[\frac{1-(1 + aL)^{1-b}}{G_o t^* a(1-b)}\right] \tag{5}$$

For a more general approach, the population density equation can be manipulated to show the effect of unsteady behavior and non-linear growth on a semilogarithm plot of the number distribution versus size.

$$\frac{\partial \ln(n)}{\partial L} = -\left[\frac{\partial \ln G}{\partial L} + \frac{1}{Gt^*} + \frac{\partial \ln(n)}{G\partial t}\right] \tag{6}$$

For steady-state, linear growth, the ln(n) versus L plot should be a straight line of slope - 1/Gt*. For transient behavior and still linear growth, the slope varies with 1/Gt* + dln(n)/Gdt. Since both G and n are functions of time and size, this results in a steeper slope for the size undergoing rapid nucleation and growth. For small t*, the first term may dominate and effective linear growth would be observed. For large t*, the unsteady-state number density term would dominate. The nonlinear behavior would be most evident with those sizes rapidly changing and would decrease with time.

In the case of non-linear growth and steady-state behavior, the slope is $-(1/Gt^*)(t^*dG/dL + 1)$. If $1 \gg t^*dG/dL$, then the slope at any value of L is $-1/Gt^*$. Thus the slope should vary with both G and t*. This may be the consequence of short residence times. If a formulation like the ASL model is valid then for small sizes ($aL \ll 1$) the growth rate is approximately independent of size. On the other hand, if $1 \ll t^*dG/dL$ then the slope should be independent of t* and vary with -dlnG/dL which, depending upon the formulation for G, may or may not change appreciably with L.

These comments as well as the results of Sharenz,[11] for transient crystallization behavior with linear growth are used to evaluate the results in this study.

Kinetic studies also yield the nucleation rate, B_o, which is the rate at which particles of zero size form. This is equal to the product of the growth rate, G_o for particles of zero size, and the nuclei distribution, n_o. This rate is a function of the supersaturation, s, of

the contents of the MSMPR, the magma density, M_T, and a constant, k_N which is a function of hydrodynamics, temperature and impurities.

$$B_0 = k_N M_T^j s^c \quad (7)$$

Since the growth rate also is considered to have a power dependence upon supersaturation (the concentration in excess of saturation divided by the saturation concentration), the nucleation rate is considered to depend upon the growth rate in the following manner

$$B_0 = k_N M_T^j G^i \quad (8)$$

for the growth rate of particle of zero size. Thus a logarithmic plot of B_0 versus G should yield a straight line with slope i, the relative nucleation order. Since B_0 equals n_0 times G_0, n_0 should vary with the growth rate to the i-1 power. Generally, the relative nucleation order is positive, although there are some system summarized in the literature that exhibit negative coefficients.[12,13]

The depiction of data as cumulative number greater than versus size does not allow differentiation between linear growth and dispersion. In order to determine which prevails, batch crystallization runs must be performed. If curves from the batch runs are somewhat symmetric, nonlinear growth rather than dispersion is indicated.[6]

EXPERIMENTAL

All of the runs were performed in a continuously stirred (600 rpm) one liter glass beaker with a glass draft tube in the center. Precipitation chemicals were introduced in the liquid near the center of the draft tube. For the MSMPR runs, liquid and crystals were discharged by gravity through a port on the side of the beaker near the liquid level. Particle size characterization was performed with a HIAC/Royco PA 720 Optical Particle Size Analyzer with the HR 1 60 HC or HR 60 HA sensor. Individual particles passing through the cell are counted and sized based upon amount of light reduction. Samples for particle size analysis were drawn from the crystallizer and diluted approximately 1/100 with filtered (2.2 micron paper) overflow. Background concentrations were determined on the filtered overflow. These values were subtracted from those measured for the diluted sample. Particles were counted in 24 size ranges, the midpoints which corresponded to 1.1, 1.3, 1.5, 1.8, 2.1, 2.5, 2.9, 3.5, 4.1, 4.8, 5.7, 6.7, 7.9, 9.4, 11.1, 13, 15.4, 18.2, 21.4, 25.3, 29.9, 35.2, 41.6, and greater than 45 microns.

The crystal density was determined by filtration of overflow through 2.2 micron paper, drying at 106^{0}C and weighing. Several series of crystallizer runs were performed. For all of the runs, ammonium hexafluorozirconate solution was prepared by dissolution of zirconium fluoride in ammonium fluoride solution. Approximately 22 g of ammonium fluoride were dissolved in hot water and 50 g of zirconium fluoride added to the solution. The resulting solution of 0.3 M ammonium hexafluorozirconate was filtered and diluted to make a working concentrations 0.1 M.

The flow rate of reactants was varied to provide residence times of 10, 30, 60 and 135 minutes. In the first series of runs and the batch runs, 0.1 M ammonium hexafluorozirconate was reacted with 0.048 M ammonium hydroxide. Equal volumes were used so that the crystallizer concentration was half of those above (about 0.05 M and 0.024 M, respectively). For each residence time, samples were periodically taken to ascertain the approach to steady- state. The pH was measured continuously during the crystallizer runs. Other runs were performed with concentrations of 0.008 M (in crystallizer) tin (IV) fluoride and a mixture of 0.05 M ammonium hexafluorizirconate and 0.008 M tin fluoride. Batch runs were also performed for the ammonium hexafluorizirconate solution. In these runs, seed was obtained from a batch crystallizer operated for 2 hours.

RESULTS

Figure 1 depicts the results from the batch runs for 0.048 M ammonium hexafluorozirconate solution. Data is reported for samples taken at various times from 1 minute up to 10 minutes. The early time samples showed a somewhat symmetrical behavior, an approximately constant increase in particle number for a given size with time for particles in the range of 2 to 12 microns. These results indicate that growth rate dispersion is not probable. They also indicate that the distribution approaches one corresponding to linear growth rate for the longer times, i.e. the curve approaches a straight line.

Figure 2 is a typical plot obtained for early times into a 30 minute residence time run. The plot is for three samples taken for 6, 7, and 8 residence times into the run. Figure 3 shows that the plot has straightened after 12, 13, and 14 residence times. Figures 4 and 5 are similar plots for the 135 minute residence time runs (after 0.5, 1.5, and 2 residence times and 3.5, 4 and 4.5 residence times respectively). Notice that insufficient elapsed time has resulted in appreciable non-linear behavior for the last figure. Data from the last figure were

fit to the nonlinear modified ASL model by with the aid of "Statgraphics" software.[14] As is sometimes done in the literature,[15,16] the ASL model was modified to equate a to 1/Gt*. Figure 6 depicts the fit for a 135 minute residence time run. The ASL model parameters obtained were: N_T = 3.5 x 10^{-14} particles/cc; b = 0.80; and G_0 = 4.86 x 10^{-5} microns/minute. The r^2 value for the data fit was 0.94. When the full ASL model was used on data averaged from the 135 minute residence time runs, the parameters were: N_T = 2.2 x 10^{13} particles/cc; a = 2.14 $micron^{-1}$; b = 1.23; and G_0 4.7 x 10^{-4} microns/minute. The r^2 value for the data fit was 0.98. Note that the value of b exceeded 1 in the last fit. This is not theoretically possible if the model fits the moment equations.[10] Notice also that the model cannot fit the "S-shaped" behavior of the plots.

Figure 7 depicts the particle diameters determined from individual runs for the 30 and 135 minute residence times as well as the 90 minute run results reported earlier in Reference 2. Notice the second order damped behavior for these sizes with time. Similar plots were reported in our previous work.[2] These results indicate that the transient behavior of the system lead to apparent nonlinear growth rate plots. Similar behavior was noted for the tin studies. Figure 8 depicts the particle diameter as a function of dimensionless time for the 10 and 30 minute tin runs. Note that the diameter oscillates without significant dampening even at large elapsed times. Figure 9 depicts a typical distribution plot for this system. Apparent non-linear growth is noted for this system as well. Once again, apparent non-linear growth may be a consequence of transient behavior.

This conclusion is born out by the results from the simulation of the low concentration tin runs by the program "Crystalball" obtained from University of Arizona.[17] Figure 10 depicts the oscillations obtained when the flow rate was doubled. Note that the particle size oscillated significantly. Figure 9 depicts the size distribution plot which also has non-linear behavior similar to that seen in the above plots. The effect of small concentrations of tin appear in Figures 11 through 15. These results are averages from three runs obtained after at least 12 elapsed residence times. Figure 11 is a plot of the magma concentration as a function of residence time and solute type. Lower yields are seen for the tin runs relative to the zirconium due to the lower tin concentration. For the longer residence times of 30 and 60 minutes the tin dramatically reduced the yield for slurries containing both tin and zirconium. Apparently the tin inhibits the crystallization of zirconium hydroxide. Figure 12 depicts growth rate information for the same runs. Mixed

results are seen here with no consistent effect of the tin on the growth rate of zirconium hydroxide. Growth rate does, however, decrease with residence time. Figure 13 depicts nuclei concentration for the runs. Here tin nuclei concentration lies above that of zirconium for the 30 and 60 minute runs. The mixture concentrations lie between the two and are significantly affected by the low tin concentration. Figure 14 shows the effect of tin concentration on particle size. The particle size for the tin runs is greater than that for the zirconium runs for the 30 and 60 minute residence times. The mixture values lie between and show a significant effect from the presence of tin. It is somewhat curious that the size and number concentrations are greater for the tin runs than for the others but the magma concentration is so much lower. This may be due to the skewness of the distributions. The tin runs have a low standard deviation for a lognormal plot of the distribution. The same is true of the mixture runs. The zirconium runs, on the other hand, have a broader distribution. Consequently there will be more of the larger sizes which contribute the most to the magma mass. Figure 15 is a plot of the logarithm of the particle concentration as a function of the logarithm of the growth rate. The slope of the zirconium runs is 0.9, the tin -7, and the mix -0.4. With approximately comparable growth rates, this indicates the birth rate of crystals in the tin system is drastically lower than the other two systems. This results in a decrease in the birth rate for the crystals in the presence of tin.

DISCUSSION OF RESULTS

Calculated saturation concentrations based upon an equilibrium solubility product of zirconium hydroxide formed from the reaction of ammonium hydroxide with hexafluorozirconate solution of 0.048 M were approximately 0.00001 M while for 0.008 M tin it was 4×10^{-7} M. Measured concentrations of zirconium and tin exiting the crystallizer were around 0.03 to 0.04 M and $2 - 6 \times 10^{-5}$ M respectively. Consequently the crystallizer solution was highly supersaturated in both species but much more so for the zirconium. The presence of tin in the mixture raised both the exiting concentration of zirconium (by about 10%) and tin (by about 100%) in the solution.

Transient behavior either from insufficient time for the system to reach steady state or from sustained oscillations, results in size distribution plots that exhibit apparent nonlinearity. Thus insufficient time for the system to reach steady-state may lead one to misinterpret the crystallization kinetics as nonlinear or exhibiting growth rate

dispersion. The system studied here exhibits linear behavior for long elapsed times and high concentrations but apparent nonlinear behavior for short times or low concentrations.

The presence of a small amount of tin resulted in a significant effect on the kinetics and yield of the zirconium hydroxide precipitation system. Slurry yield decreased, while both particle size and number concentration increased. The tin also apparently resulted in decreased birth rates.

CONCLUSIONS

The following conclusions can be made based upon the results of the study.

1. Particle distributions and sizes can be approximately modeled employing the McCabe Linear growth model. Apparent nonlinear behavior is a consequence of unsteady-state kinetics.

2. Particle size and/or slurry concentrations should be monitored to ensure steady-state is achieved before attempting to determine steady-state kinetic information from experimental data.

3. For low concentrations, extended times may be required for the system to reach steady-state. Significant oscillatory behavior in particle size evidences this.

4. Small amounts of tin significantly effect the kinetics of zirconium hydroxide precipitation. Significant reductions in yield were observed.

REFERENCES

1. N. A. Chipman and T. E. Carleson, Evaluation of a Modified Zirflex Process to Minimize High-Level Waste Generation at the Idaho Chemical Processing Plant, WINCO-1039 (June 1987).

2. T. E. Carleson and N. A. Chipman, "Nucleation and Growth Kinetics of Zirconium Hydroxide by Precipitation with Ammonium Hydroxide", Presented at the 1987 Annual AIChE Meeting, New York, New York, WINCO-M-11332 (November 1987).

3. D. C. Timm and M. A. Larson, "Effect of Nucleation Kinetics on The Dynamic Behavior of a Continuous Crystallizer", AIChE Journal, Vol. 14, No. 3 (1968).

4. D. C. Murray and M. A. Larson, "Size Distribution Dynamics in a Salting Out Crystallizer", AIChE Journal, Vol. 11, No. 4 (1965).

5. K. Akoglu, N. S. Tavare, and J. Garside, "Dynamic Simulation of a Non-Isothermal MSMPR Crystallizer," Chem. Eng. Commun., Vol. 29 (1984).

6. A. D. Randolph and M. A. Larson, Theory of Particulate Processes, 2nd Edition, Academic Press, Inc., San Diego, CA (1988).

7. R. C. Zumstein and R. W. Rousseau, "Growth Rate Dispersion by Initial Growth Rate Distributions and Growth Rate Fluctuations", AIChE Journal, Vol. 33, No. 1 (1987).

8. A. D. Randolph and E. T. White, "Modeling Size Dispersion in the Prediction of Crystal Size Distribution", Chem. Eng. Sci., Vol 32 (1977).

9. K. A. Berglund and M. A. Larson, "Growth of Contact Nuclei of Citric Acid Monohydrate", AIChE Symposium Series, No. 215, Vol. 78 (1982).

10. C. F. Abegg, J. D. Stevens, and M. A. Larson, "Crystal Size Distributions in Continuous Crystallizers When Growth Rate is Size Dependent", AIChE Jornal, Vol. 14, No. 1 (1968).

11. R. Sharenz, "Dynamic Simulation and Control of Crystal Size Distribution in a Complex Crystallizer", M.S. Thesis University of Arizona, Tucson, Arizona (1987).

12. J. Garside and M. B. Shah, "Crystallizer Kinetics from MSMPR Crystallizers", Ind. Eng. Chem. Process Des. Dev., Vol. 19, No. 4 (1980).

13. H. Yagi, et.al., "Crystallization of Calcium Carbonate Accompanying Chemical Adsorption," AIChE Journal, Vol. 33, No. 1, (1987).

14. Statgraphics®, STSC Inc, Rockville, MD (1988).

15. S. Jancic and J. Garside, "A New Technique for Accurate Crystal Size Distribution Analysis in an MSMPR Crystallizer", Industrial Crystallization, Plenum Press, New York, New York, J. W. Mullin, Ed. (1976).

16. F. P. O'Dell and R. W. Rousseau, "Magma Density and Dominant Size for Size Dependent Crystal Growth", AIChE Journal, Vol. 24, No. 4 (1978).

17. R. Sharenz, "CRYSTALBALL II©", University of Arizona, Tuscon, Arizona (1987).

DISCLAIMER

Figure 1

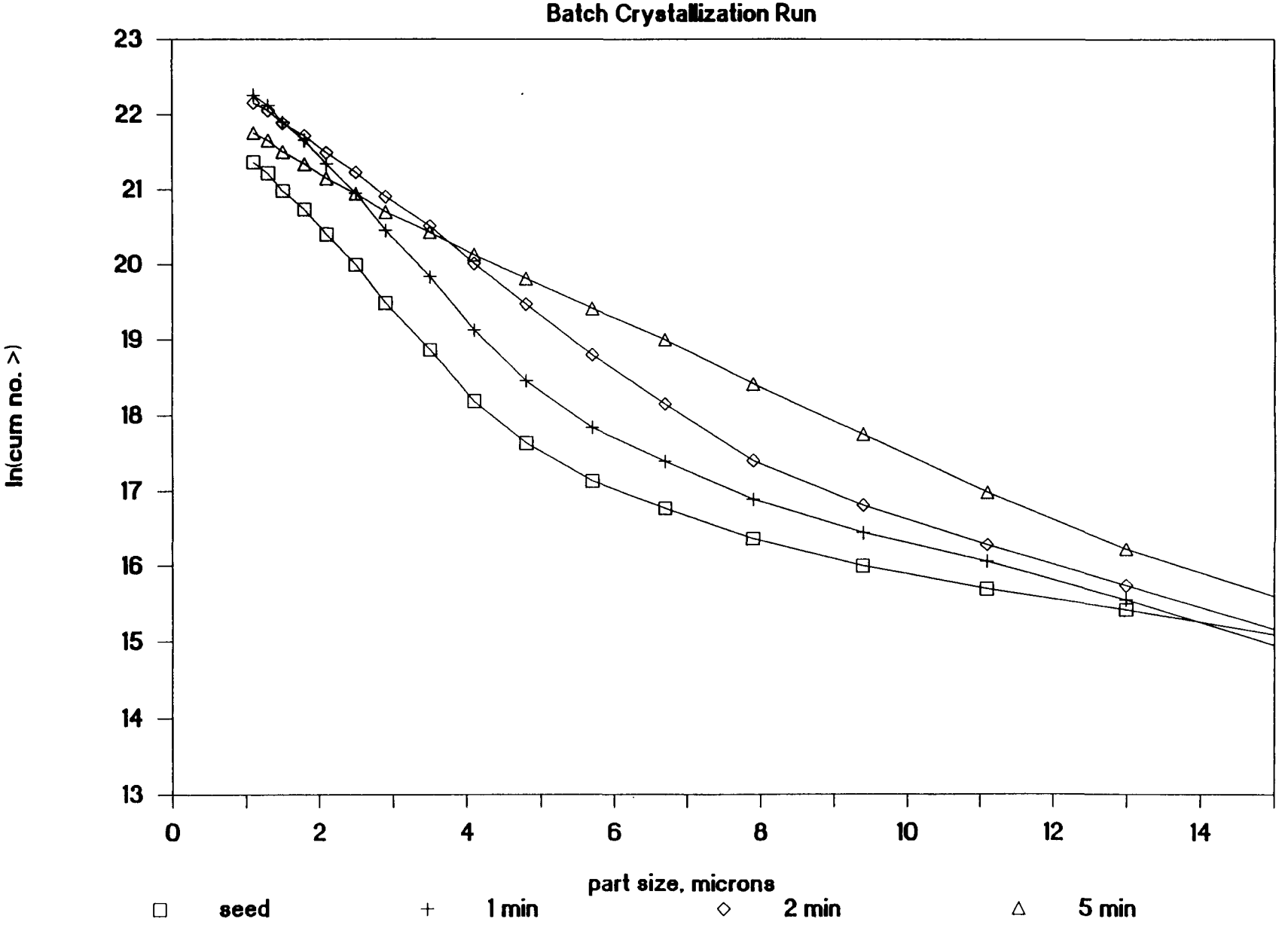
Batch Crystallization Run
ln(cum no. >)
23
22
21
20
19
18
17
16
15
14
13
0
2
4
6
8
10
12
14
part size, microns
seed
1 min
2 min
5 min

Figure 2

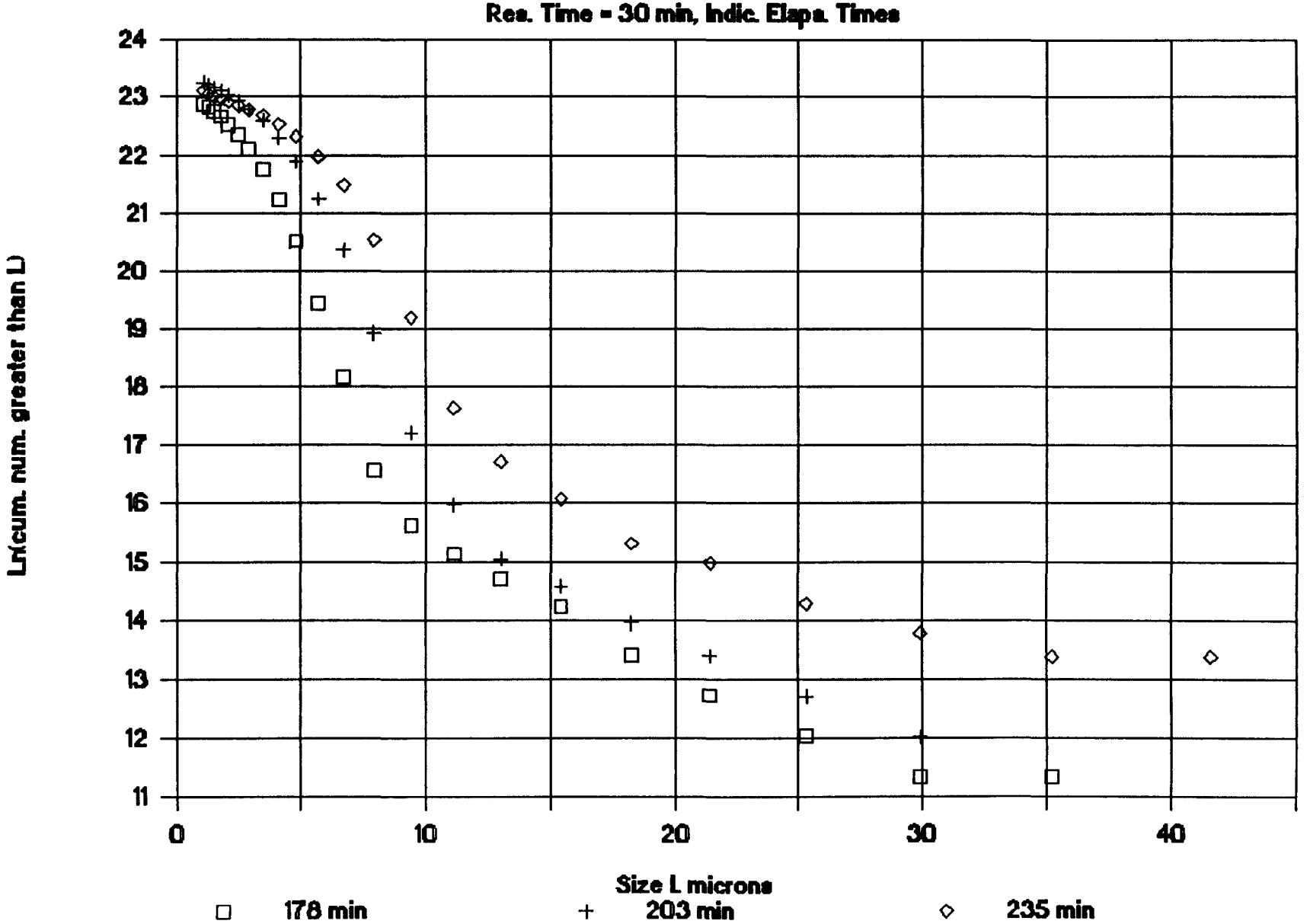
Res. Time = 30 min, Indic. Elaps. Times
Ln(cum. num. greater than L)
24
23
22
21
20
19
18
17
16
15
14
13
12
11
0
10
20
30
40
Size L microns
178 min
203 min
235 min

Figure 3

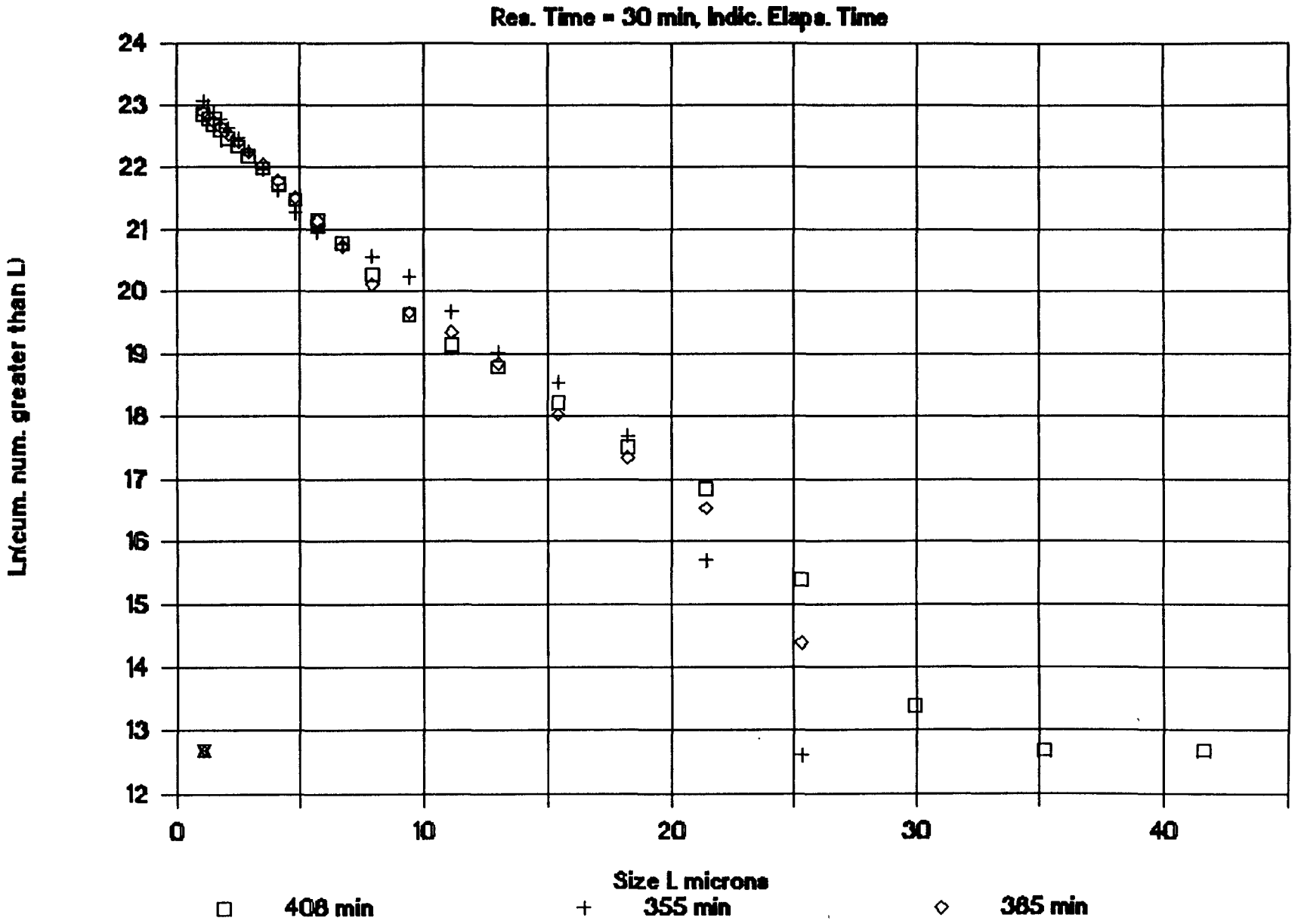
Res. Time = 30 min, Indic. Elaps. Time
Ln(cum. num. greater than L)
24
23
22
21
20
19
18
17
16
15
14
13
12
0
10
20
30
40
Size L microns
408 min
355 min
385 min

Figure 4

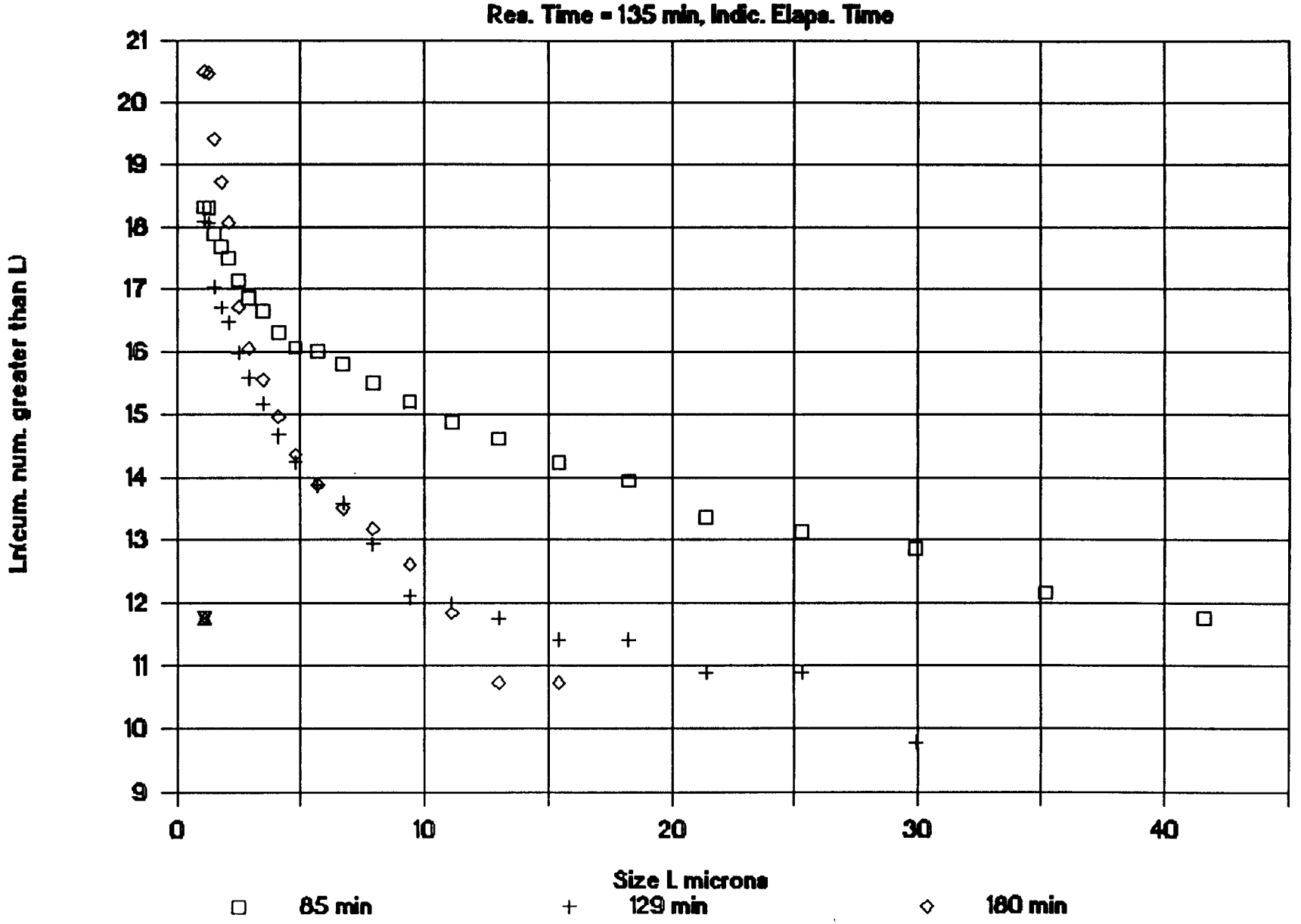
Res. Time = 135 min, Indic. Elaps. Time
Ln(cum. num. greater than L)
21
20
19
18
17
16
15
14
13
12
11
10
9
0
10
20
30
40
Size L microns
85 min
129 min
180 min

Figure 5

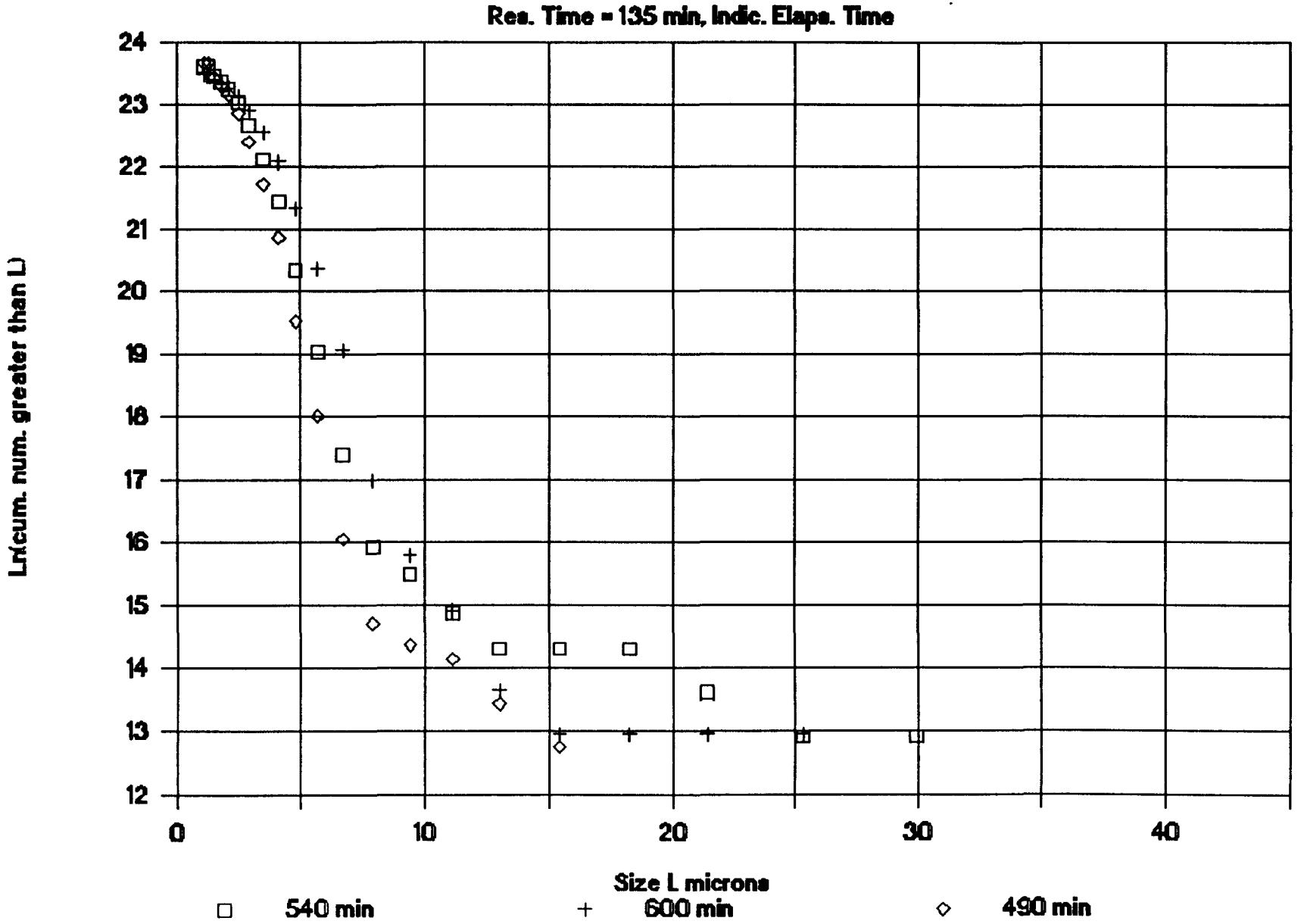
Res. Time = 135 min, Indic. Elaps. Time
Ln(cum. num. greater than L)
24
23
22
21
20
19
18
17
16
15
14
13
12
0
10
20
30
40
Size L microns
540 min
600 min
490 min

Figure 6

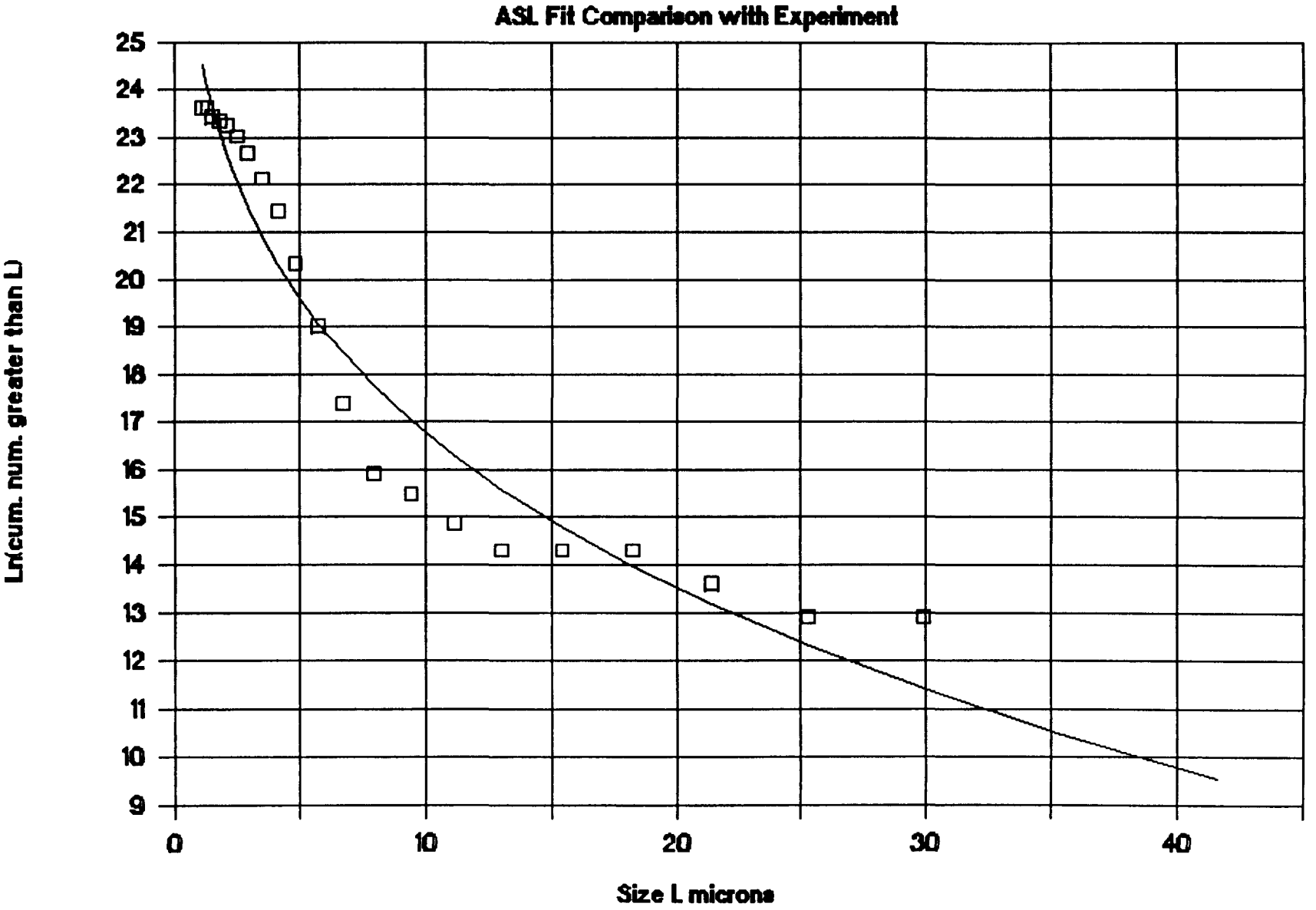
ASL Fit Comparison with Experiment
Ln(cum. num. greater than L)
25
24
23
22
21
20
19
18
17
16
15
14
13
12
11
10
9
0
10
20
30
40
Size L microns

Figure 7

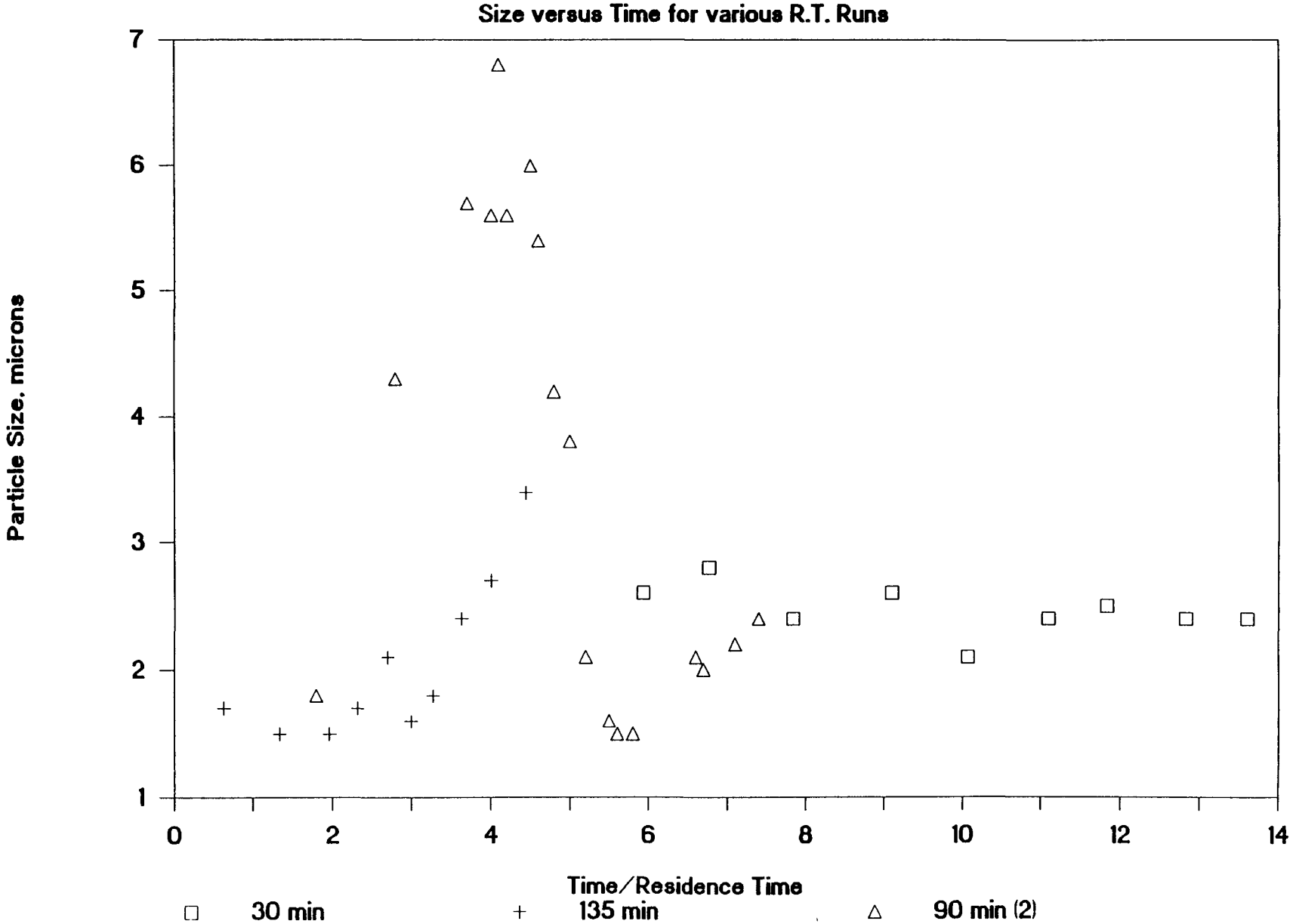
Size versus Time for various R.T. Runs
Particle Size, microns
7
6
5
4
3
2
1
0
2
4
6
8
10
12
14
Time/Residence Time
30 min
135 min
90 min (2)

Figure 8

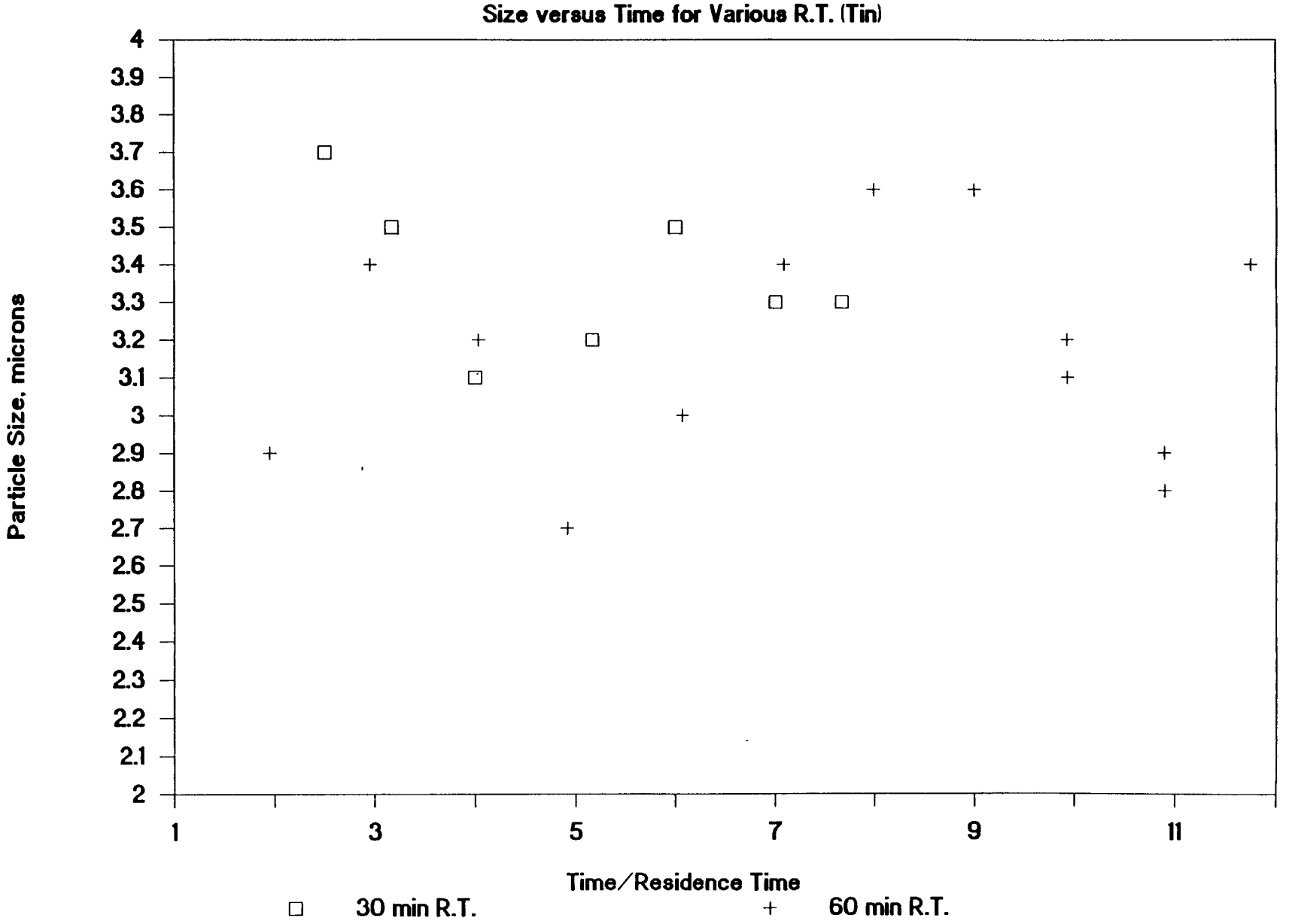
Size versus Time for Various R.T. (Tin)
Particle Size, microns
4
3.9
3.8
3.7
3.6
3.5
3.4
3.3
3.2
3.1
3
2.9
2.8
2.7
2.6
2.5
2.4
2.3
2.2
2.1
2
1
3
5
7
9
11
Time/Residence Time
30 min R.T.
60 min R.T.

Figure 9

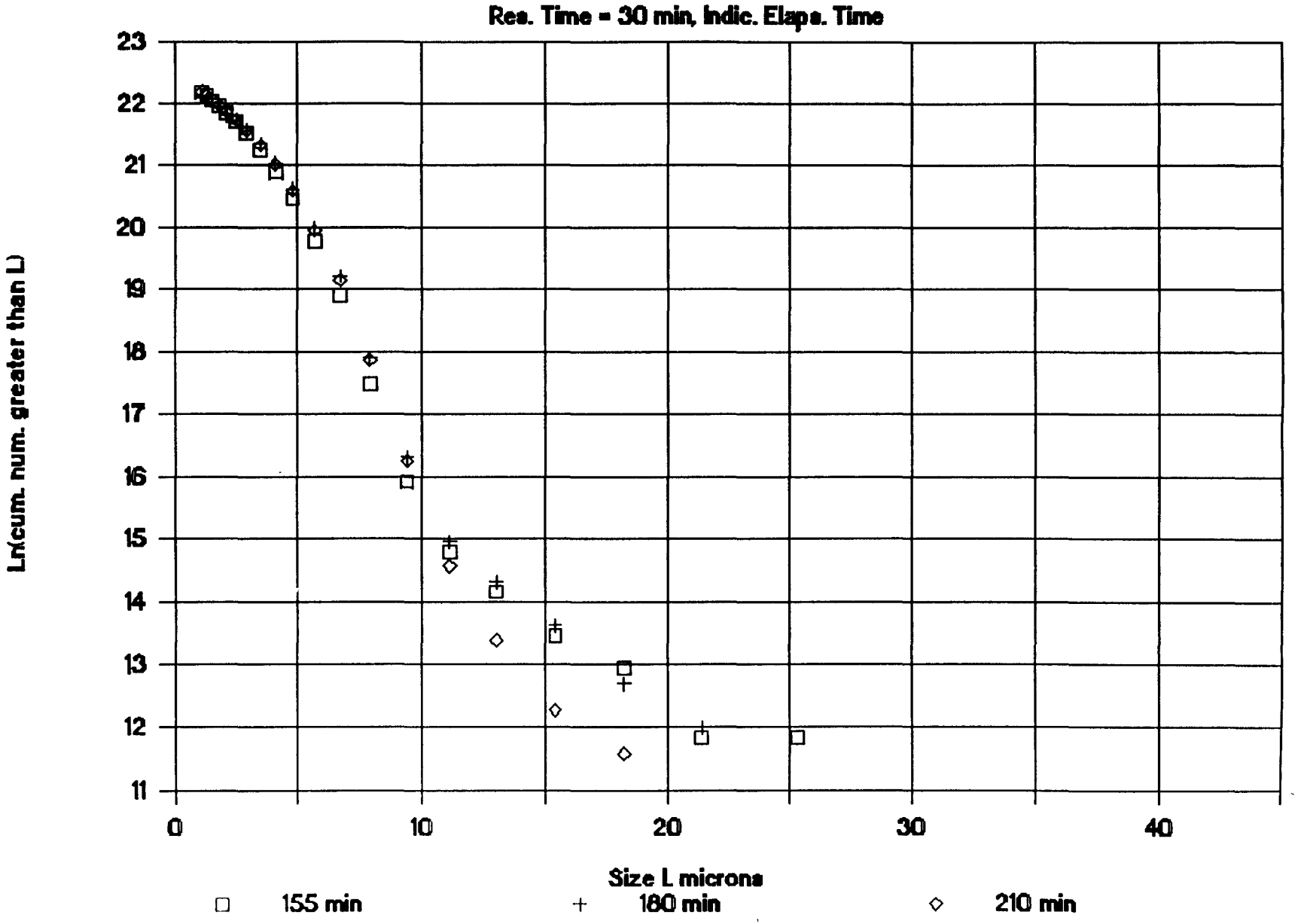
Res. Time = 30 min, Indic. Elaps. Time
Ln(cum. num. greater than L)
23
22
21
20
19
18
17
16
15
14
13
12
11
0
10
20
30
40
Size L microns
155 min
180 min
210 min

Figure 10

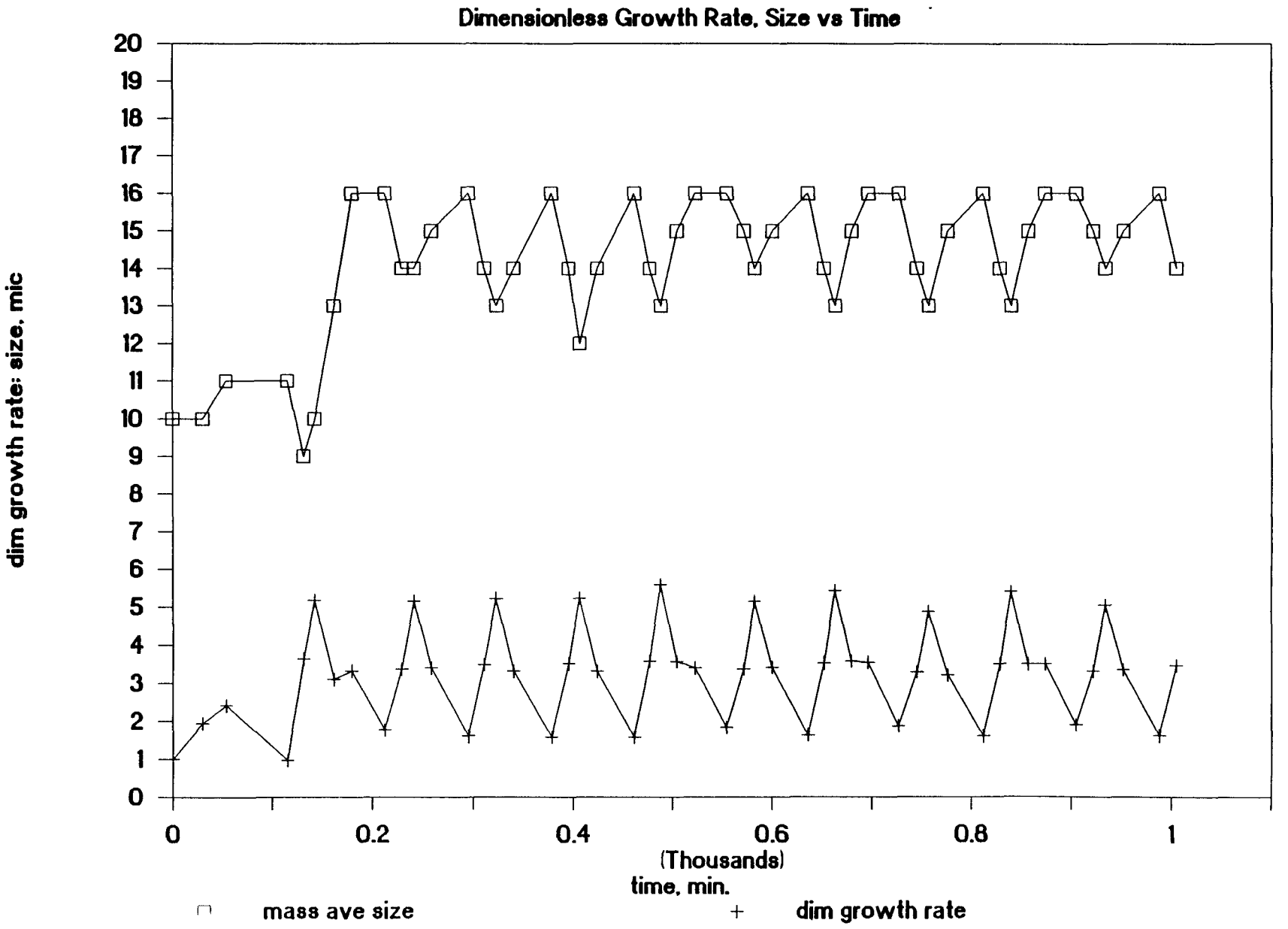
Dimensionless Growth Rate, Size vs Time
dim growth rate: size, mic
20
19
18
17
16
15
14
13
12
11
10
9
8
7
6
5
4
3
2
1
0
0
0.2
0.4
0.6
0.8
1
(Thousands)
time, min.
mass ave size
dim growth rate

Figure 11

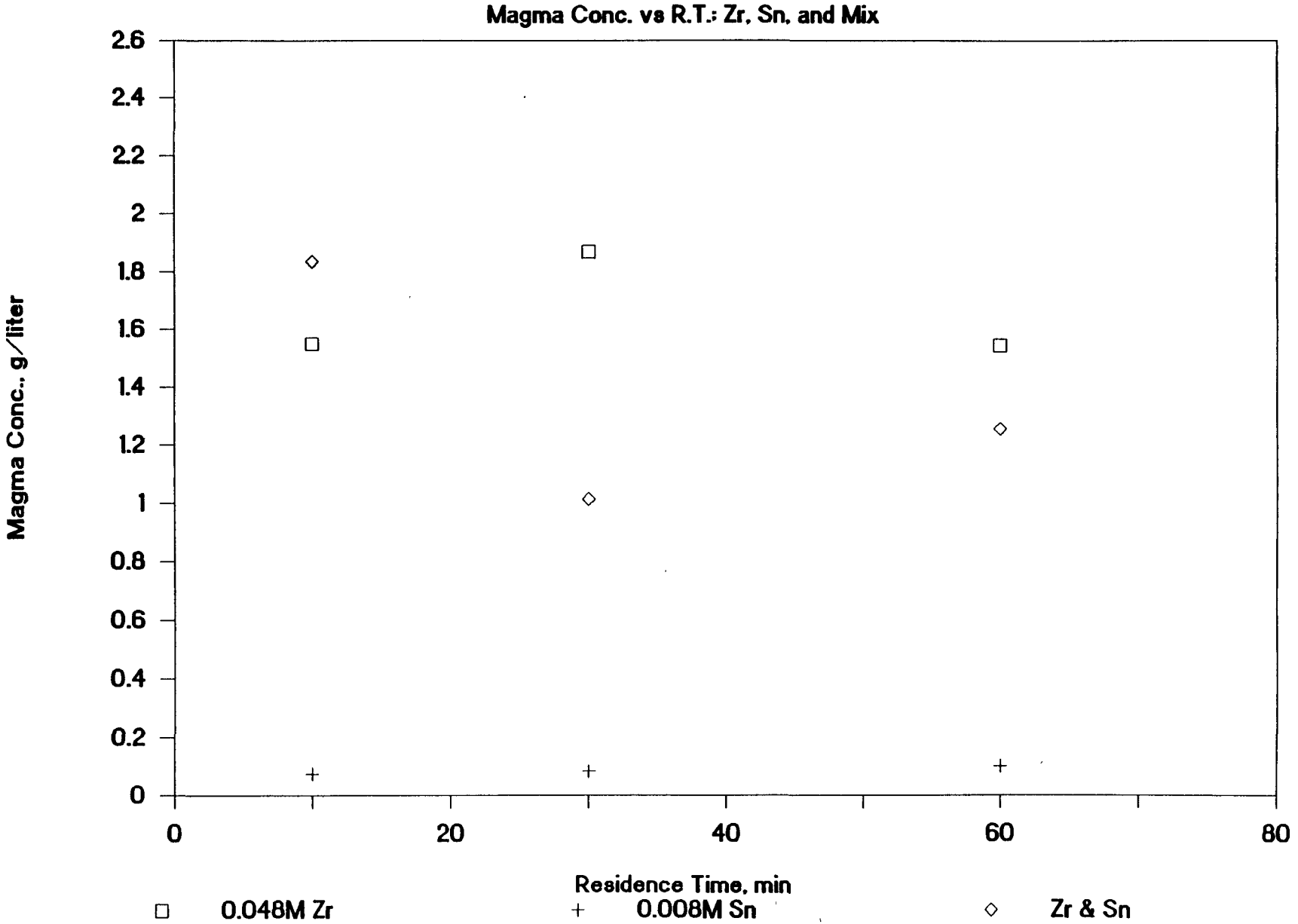
Magma Conc. vs R.T.: Zr, Sn, and Mix
Magma Conc., g/liter
2.6
2.4
2.2
2
1.8
1.6
1.4
1.2
1
0.8
0.6
0.4
0.2
0
0
20
40
60
80
Residence Time, min
0.048M Zr
0.008M Sn
Zr & Sn

Figure 12

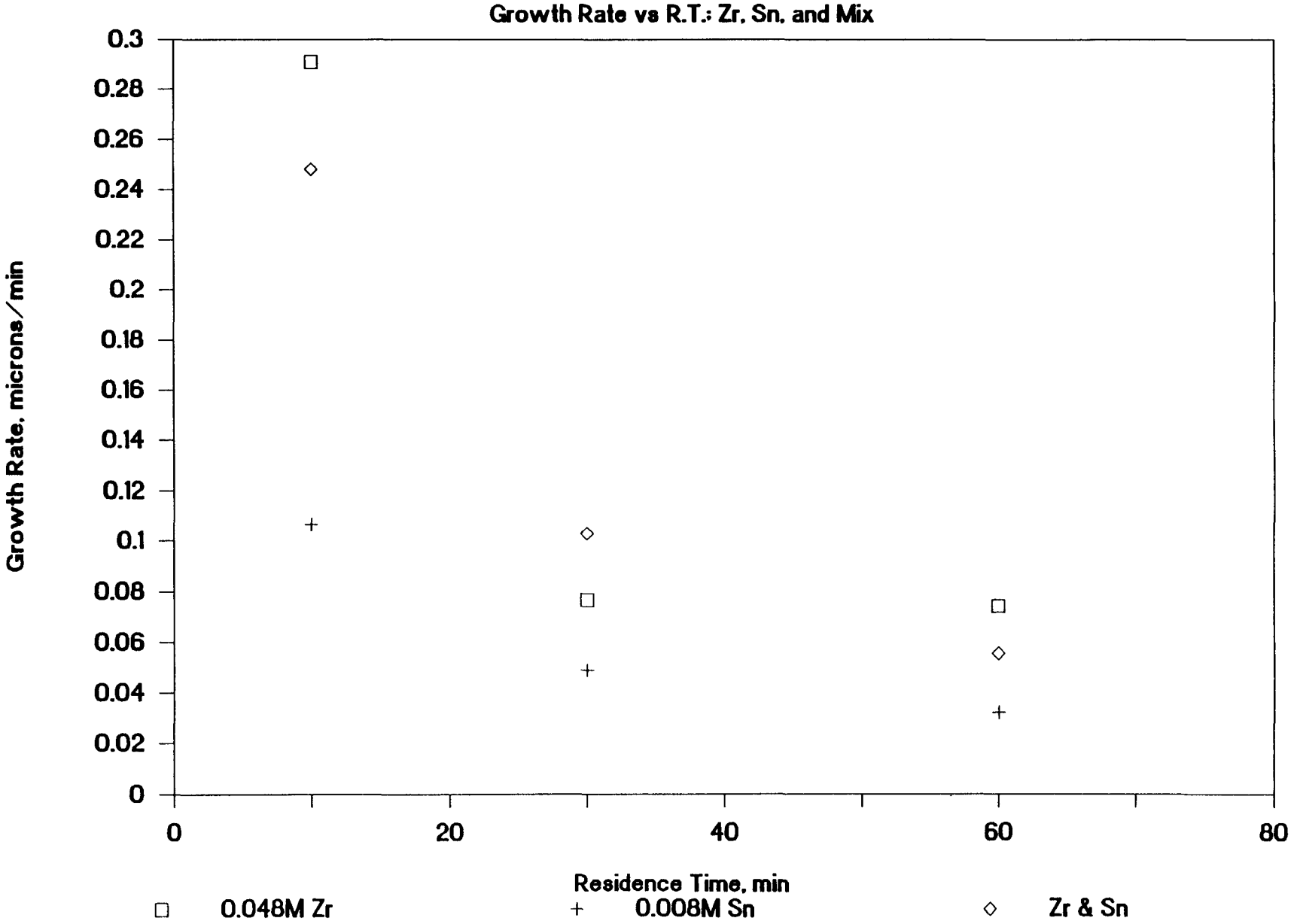
Growth Rate vs R.T.: Zr, Sn, and Mix
Growth Rate, microns/min
0.3
0.28
0.26
0.24
0.22
0.2
0.18
0.16
0.14
0.12
0.1
0.08
0.06
0.04
0.02
0
0
20
40
60
80
Residence Time, min
0.048M Zr
0.008M Sn
Zr & Sn

Figure 13

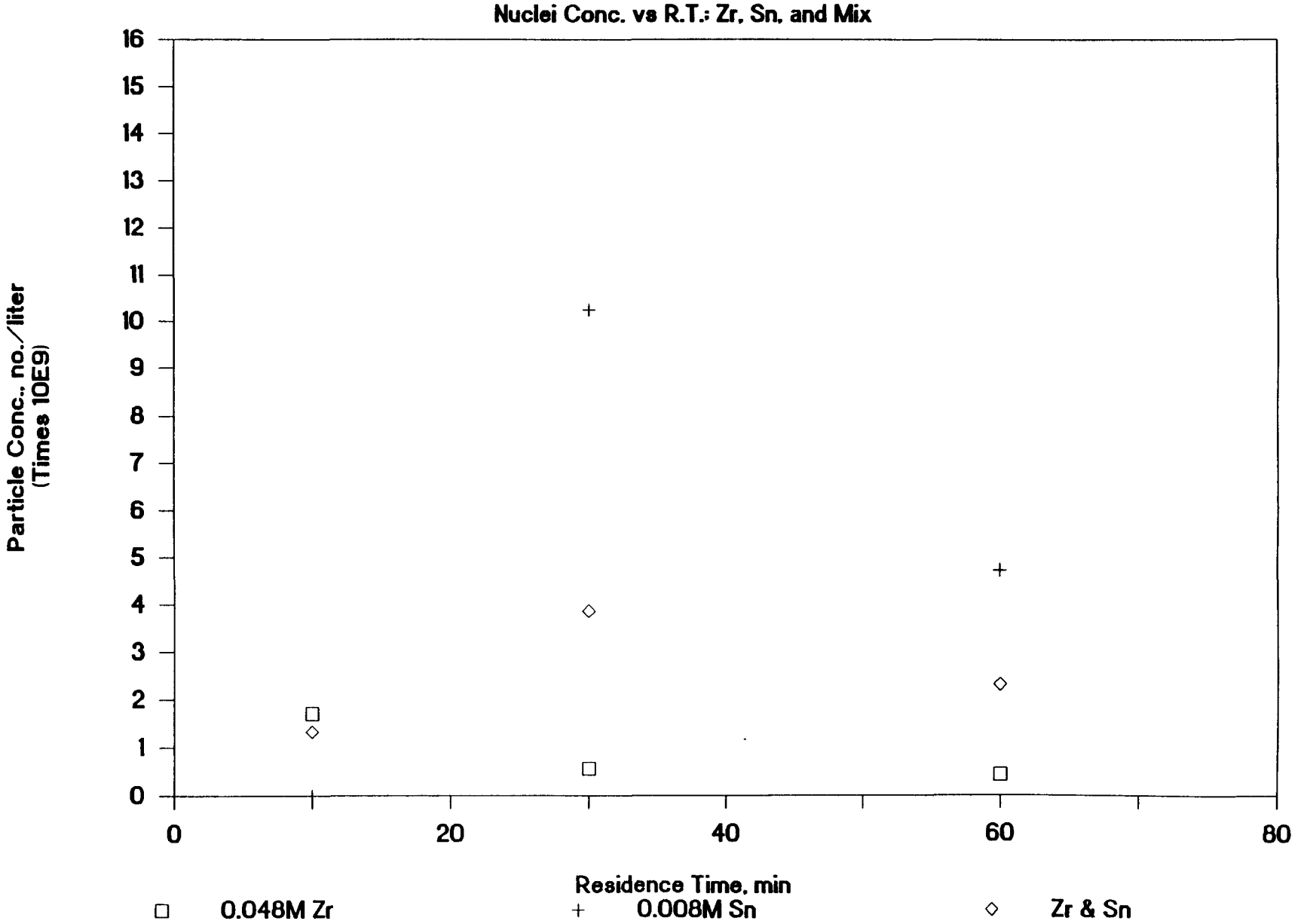
Nuclei Conc. vs R.T.: Zr, Sn, and Mix
Particle Conc., no./liter
(Times 10E9)
16
15
14
13
12
11
10
9
8
7
6
5
4
3
2
1
0
0
20
40
60
80
Residence Time, min
0.048M Zr
0.008M Sn
Zr & Sn

Figure 14

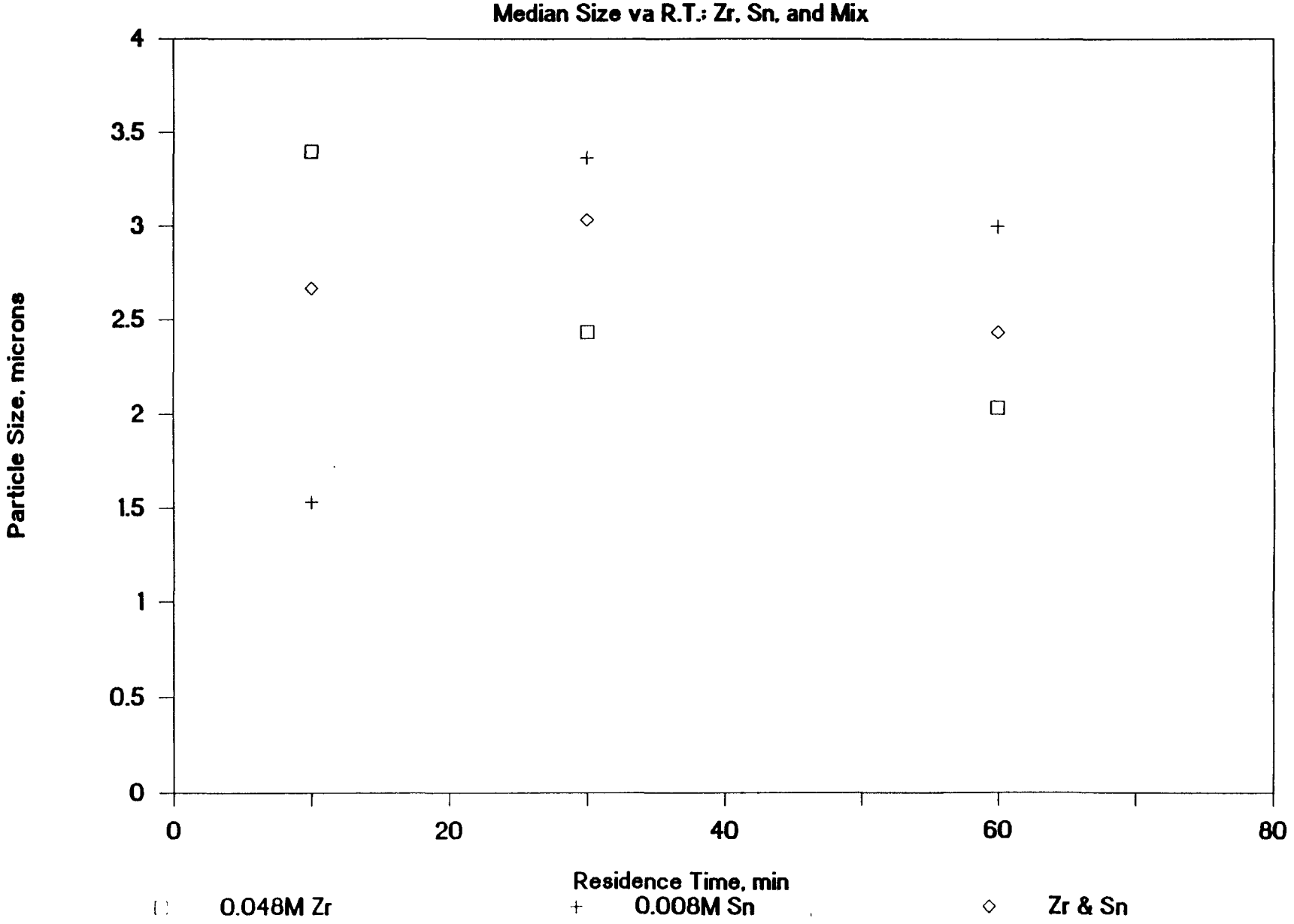
Median Size va R.T.: Zr, Sn, and Mix
Particle Size, microns
4
3.5
3
2.5
2
1.5
1
0.5
0
0
20
40
60
80
Residence Time, min
0.048M Zr
0.008M Sn
Zr & Sn

Figure 15

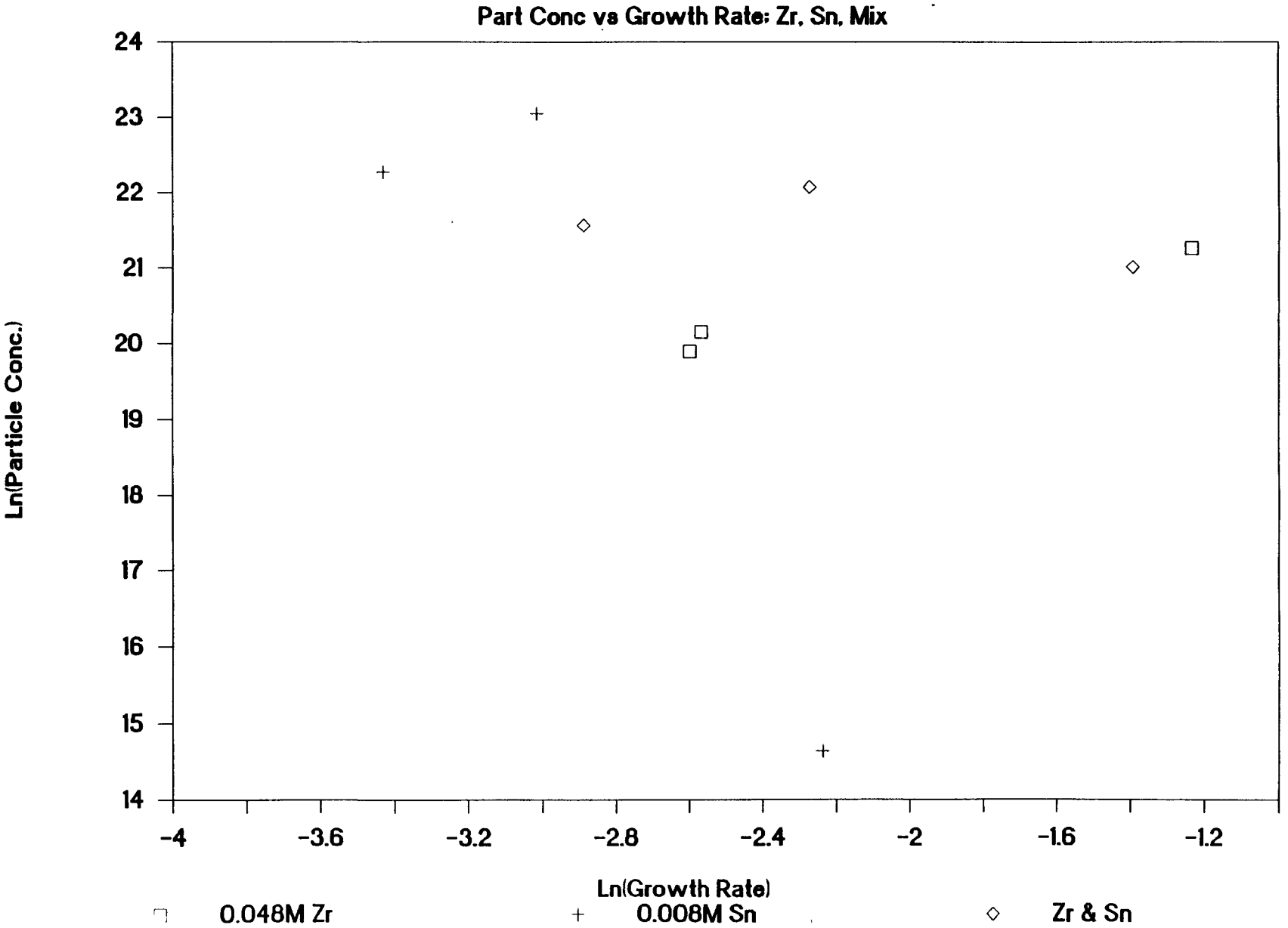
Part Conc vs Growth Rate: Zr, Sn, Mix
Ln(Particle Conc.)
24
23
22
21
20
19
18
17
16
15
14
-4
-3.6
-3.2
-2.8
-2.4
-2
-1.6
-1.2
Ln(Growth Rate)
0.048M Zr
0.008M Sn
Zr & Sn